

Investigating Blue Straggler Production through Binary Star Evolution

Matthew W. Bailey¹, Robert D. Mathieu², Aaron M. Geller³, Jarrod R. Hurley^{4,5}, Tracy M. Hodge⁶

Abstract

Mathieu et al. (2009) has found that among the 21 blue stragglers of NGC 188 (7 Gyr), 16 are in spectroscopic binaries. Furthermore, most of these binaries have periods near 1,000 days. Hole et al. (2009) has found that among 12 blue stragglers of NGC 6819 (2.4 Gyr), only 4 are in binary. We have used simulations of binary evolution from the Zero Age Main Sequence to 7 Gyrs and 2.4 Gyrs to determine whether binary evolution could reproduce the quantity of NGC 188 and NGC 6819 blue stragglers. We addressed this question through a Monte Carlo approach. We created many realizations of a population of 10,000 binary stars with the eccentricity, period and secondary mass distributions found by Duquennoy & Mayor (1990) for field binaries. This population was then synthetically evolved with the Binary Star Evolution (BSE) algorithm of Hurley et al. (2002) to an age of 7 Gyrs and 2.4 Gyrs, respectively. The blue stragglers were selected from the resulting population photometrically by luminosity and B-V color. The 7.0 Gyr simulation produced on average 4-5 BSs, with a 57% binary fraction, while the 2.4 Gyr simulation produced 5 BSs with a 48% binary percentage. For the 7 Gyr simulation, the immediate conclusion is that the period distribution of NGC 188 blue stragglers can be produced by internal binary processes as modeled by BSE. However, all of the 1000-day period blue straggler binaries were the result of wind accretion. As such, the typical increase in mass of a primary star (the blue straggler) was low, and the CMD distribution of the simulated blue stragglers was more constrained to near the cluster turnoff than the actual blue stragglers. Binary orbits have yet to be resolved for the NGC 6819 BSs, however similar regionalization near the turnoff for simulated BSs with similar periods was found.

¹ Berea College, CPO 092 Berea, KY 40404

² Department of Astrophysics University of Wisconsin - Madison 5534 Sterling Hall 475 N. Charter Street, Madison WI 53706-1582

³ Department of Astrophysics University of Wisconsin - Madison 5534 Sterling Hall 475 N. Charter Street, Madison WI 53706-1582

⁴ Centre for Stellar and Planetary Astrophysics, School of Mathematical Sciences, Monash University, VIC 3800, Australia

⁵ Department of Astrophysics, American Museum of Natural History, Central Park West at 79th Street, New York, NY 10024, USA

⁶ Department of Physics, Berea College, CPO2191 Berea, KY 40404

1. Introduction

1.1 Single Star Evolution

Analysis of stellar spectra provide information that the atmospheres of most stars are composed primarily of hydrogen, approximately 70 % by mass (Ostlie and Carroll 2007). Assuming that the initial composition of a star is homogeneous then the conversion of hydrogen to helium via nuclear fusion should be the first reactions to occur within the star. Alternatively, since the associated Coulomb barrier for hydrogen nuclei is lower than that of more massive nuclei, hence resulting in fusion at the lowest possible temperature, these reactions *should* occur first. Hydrogen burning is a slow process. In fact, Ostlie and Carroll (2007) predict that the hydrogen burning lifetime for the sun is on the order of 10 billion years. Consequently, because of the predominance of hydrogen that initially exists in the core, the interior composition and structure of the star will change slowly. According to the *Vogt – Russell Theorem*, any change in composition or mass requires a readjustment of the effective temperature and luminosity. In other words, the observational characteristics of the star must change as a consequence of the central nuclear reactions (Ostlie and Carroll 2007).

A fundamental tool in the understanding of stellar evolution is the Hertzsprung Russell Diagram (HRD) which relates the observable stellar properties of luminosity, L , and effective surface temperature, T_{eff} (Hurley et al 2000). Any star which burns hydrogen in its core is said to a *Main Sequence* (MS) star. According to Ostlie and Carroll (2007), MS luminosities can range from 5×10^{-4} solar Luminosity to approximately 1×10^6 solar luminosity, a range of nine orders of magnitude. The range in stellar masses on the other hand, typically extends across only three orders of magnitude for MS stars. Such an imbalance of luminosity to mass demonstrates the enormous rate of energy output from upper MS stars, to lower ones. Upper MS stars, with higher mass and luminosities in figure 1, therefore consume their hydrogen in a much shorter period of time. In general, MS lifetimes are inversely proportional to luminosity, or equivalently, MS lifetimes are inversely proportional to the star's mass.

The age of a star is measured from the *zero-age main sequence (ZAMS)* which is defined by the implied diagonal line in the HRD where stars of various masses first reach the MS and begin equilibrium core hydrogen burning (Ostlie and Carroll 2007). Figure 1 shows the evolution of a selection of stars in the HRD from the ZAMS until exhaustion of their core hydrogen supply. Once core hydrogen is depleted, the star is no longer a MS star. According to Hurley et al. (2000), During core hydrogen burning on the MS, low mass stars move upwards in L, and to higher T_{eff} on the HRD, while higher mass stars will also move upwards in L but to a region of lower T_{eff} . For stars of all masses, post MS evolution leads ultimately to

decreasing T_{eff} . This is due in part to the swelling of the outer envelope of the star as it ascends the next stage in evolution known as the Giant Branch (GB) (Hurley et al. 2000).

Furthermore, Hurley et al. (2000) suggests that a low-mass star's size will continue to expand as they evolve off the MS, though more gradually than stars of higher mass. Various stages of evolution proceed beyond the GB, however for the ensuing discussion the cogent point is this, core hydrogen burn defines a main sequence star and subsequent evolutionary stages are a direct result of the star's mass. To change the mass of a star at any point in time is to change the state of the star's evolution.

1.2 Star Clusters

According to Ostlie and Carroll (2007), at least half of all the stars in the sky are contained in multiple systems, meaning two or more stars in orbit about a common center of mass. This implies about half of all stars will age in an environment uninhabited by nearby stars

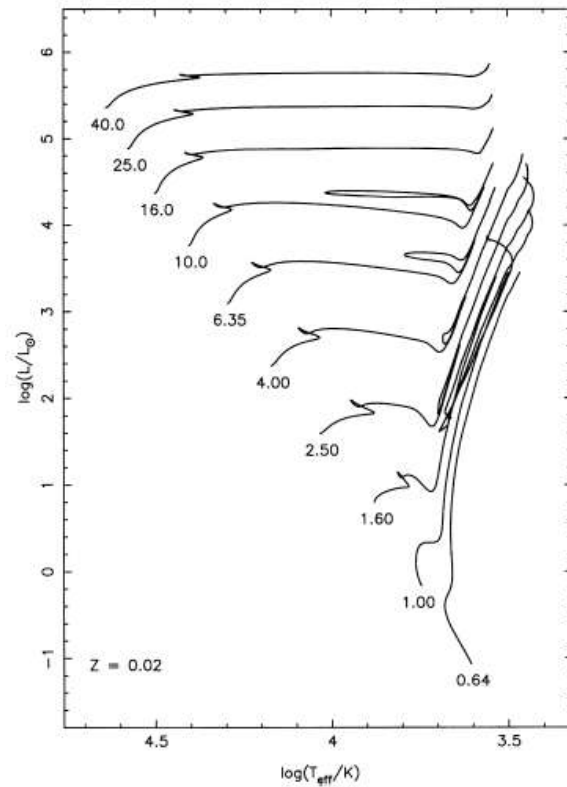


Figure 1. The evolution stars in the HRD for masses 0.64, 1.0, 1.6, 2.5, 4.0, 6.35, 10, 16, 25, and 40 solar masses from the zero-age main sequence (ZAMS), where a star adjusts itself to nuclear burning equilibrium, until the end of their nuclear burning lifetimes. The left most upward diagonal defines the main sequence. Diagram by Hurley et al. (2000)

whereas the remainder exists in the presence of neighboring stars. Depending upon their orbital separation, these multiple stars may exhibit vastly differing evolutionary stages than possible from standard evolutionary tracts of single stars (Ostlie and Carroll 2007). Before venturing into the mechanisms of binary star evolution, a brief overview of star cluster formation will be presented along with the nomenclature and tools utilized to obtain information about these clusters and their environments.

Stars are formed from the interstellar medium (ISM), and eventually return their material back to it through stellar winds, by the ejection of planetary nebulae, or through supernova explosions (Ostlie and Carroll 2007). Unlike the material from which the stars were initially formed, the material that is given back to the ISM has been enriched with heavier elements that were produced through the various phases of nuclear reactions governing the star's life. Succeeding generations of stars are therefore composed of higher concentrations of heavy elements than did their ancestors and are hence referred to as metal rich or *Population I* stars (Ostlie and Carroll 2007).

During the collapse of a molecular cloud, stellar clusters can form, ranging in size from tens of stars to hundreds of thousands of stars (Ostlie and Carroll 2007). There are two chief categorizations of clusters, namely *globular clusters* and galactic or *open clusters*. Globular clusters are old, having formed when the Galaxy was very young. Stryker (1993) suggests that they are some of the oldest objects in the Milky Way. They also contain the largest number of stars, from as few as ten thousands, upwards of one million members. Population I clusters, such as NGC – 188 and the Pleiades, are typically smaller and younger. The smaller open clusters, range from 10 – 10,000 stars, typically forming in arms of spiral galaxies (Ostlie and Carroll 2007). According to Ostlie and Carroll, every member of a given cluster formed from the same cloud and therefore has approximately equal compositions, forming likewise at approximately the same time. If one excludes processes such as membership in a binary system for reasons which will be discussed later, then according to the Vogt-Russell theorem, the differences in evolutionary states between the various stars of the cluster are due solely to their initial mass (Ostlie and Carroll 2007). Clusters are therefore valued because a variety of stellar masses are present, hence for sufficiently large clusters, at any given moment in time, the dependence of evolution as a function of stellar mass can be observed, primarily through a plot called a *color magnitude diagram*.

1.3 Color Magnitude Diagrams

In order to study the life cycle of stars, it is advantageous to know the age of the observed stars. Stellar clusters provide such an opportunity to deduce the ages of member stars. Normally, the HRD plots the *spectral type* or temperature of a star against the star's intrinsic luminosity, or brightness. A star's spectral type is deduced from the relative strength of the stars atomic absorption lines found by taking a star's spectrum and are related to the star's color – higher T_{eff} corresponding to bluer stars and lower T_{eff} to redder stars (Ostlie and Carroll 2007). A star's temperature can also be measured by determining its radiant flux through two different color filters – blue and green are common. Plotting the brightness of a star its versus color, which is measured in units of *apparent magnitudes*, therefore serves as a way to construct an HRD without taking the spectrum of the star. Such a plot of an entire cluster of stars yields what is called a *color-magnitude diagram* (CMD).

Color magnitude diagrams of clusters are invaluable in the study of stellar evolution, as they offer the ability to test current theories for each stage throughout the life cycle of stars. Since core – hydrogen burning lifetimes are inversely related to mass, Ostlie and Carroll (2007) explain that continued evolution of the cluster means that the *main sequence turnoff* point identified by the kink at the top of the MS where stars in the cluster are currently leaving the main sequence, become redder and less luminous with time. As a result, Geller et al (2008) provides an estimate of the age of the open cluster NGC 188 by the location of the uppermost point of its main sequence to be 7 billion years old.

1.4 Blue Straggler Stars

According to Stryker (1993) Blue Straggler stars (BSs) are found in all populations in the field, in open clusters of all ages, as well as in globular clusters. BSs are characterized primarily by their atypical position above and *blueward* of the main sequence turnoff on a CMD (Stryker 1993; Geller et al. 2008; Hole et al. 2009). Stryker adds that if the BSs had been a normal single star, explainable by standard stellar evolution, then they should not populate this region of the CMD. According to Stryker (1993), these stars should have evolved away from the main sequence, migrating with the majority of the cluster stars to redder color (or cooler temperatures) as they commence the giant branch phase of evolution. This follows from the theory of core –

hydrogen burning mentioned in the previous description of main sequence evolution by Ostlie and Carroll (2007).

Stryker (1993) adds that early thoughts to explain the straggling population were that these BSs might be field stars; stars that lie in the line of sight of the cluster and perceived as cluster members mistakenly. Since then, proper motion studies, (Cudworth 1985; Mathieu & Latham 1986; Geller et al 2008), indicate that BSs are probable members within their respective cluster.

Whether they are single or binary, Stryker (1993) asserts the existence of BSs point to an incomplete understanding of stellar evolution and possibly of star formation within clusters. Modeled as single stars, Stryker (1993) claims that studies of BSs necessarily involve processes deep in the energy generation regions for which observational constraints on energy generation mechanisms have been traditionally difficult to acquire (Stryker 1993). On the other hand, mounting evidence seems to convey that BSs in perhaps all systems but the youngest are the results of binary star evolution (Collier and Jenkins 1984; Mathieu and Latham 1986; Mateo et al. 1990; Geller et al. 2008). If this is true, then Stryker (1993) maintains that BSs are of utmost value for their ability to serve as tracers of binary populations along with the ability to discern how binary interactions affect the evolutionary courses of each star along with the system as a whole. Such is the purpose of this study, to examine current binary star evolution theory and its ability to recreate BSs populations in observed open clusters.

1.5 Differences in Binary Star Evolution and Single Star evolution

If a binary is separated by a sufficiently large distance then single star evolution is adequate to explain each star's evolutionary track. If the binary members become close, then according to Hurley et al (2002), interactions can occur with consequences on the orbital parameters such as period and eccentricity; the physical appearance of the stars may be changed similarly. The Binary Star Evolution algorithm (BSE) of Hurley et al. (2002) describes the various mechanisms behind these interactions, and the diverse results that can occur. While it is not the goal here to explain the BSE in detail, the following information merely highlights some of its areas considered pertinent for the progress of the study.

1.5.1 Effects of tides

In close binary systems, observations find that stellar rotation synchronizes with the orbital motion (Levato 1974). In order to synchronize, Hurley et al. (2002) suggests that the stars do not necessarily need to be in contact though their proximity to one another must be such that friction from the interacting tidal forces can dissipate orbital energy. In addition, the degree of tidal interaction is dependent upon the ratio of the stellar radius to the separation distance between the stars (Hut 1981).

According to Hurley et al. (2002), the presence of a companion introduces a tidal or differential force that acts to elongate the star along the line between the center of mass, which produces a tidal bulge. If the rotational period of the star is shorter than the orbital period, then frictional forces on the surface of the star will drag the bulge axis ahead of the line of centers. As the stars orbit each other, the resulting tides of the stars will tend either lag or precede the line of centers, which as Hurley emphasizes, produces a torque on the system. This torque transfers angular momentum between the stellar spin and the orbit, ultimately dissipating orbital energy. As energy dissipates through the tides, the total energy of the binary system diminishes, thus changing the orbital parameters of the binary (Hurley et al. 2002). Ultimately, Hut (1980) explains that the stars may approach an equilibrium state or spiral inwards until *merger*. The equilibrium state is characterized by co-rotation and a circular orbit, corresponding to a minimum energy for a given total angular momentum and alignment of the spin – orbit axes. Other angular momentum loss mechanisms specific to binary systems such as gravitational radiation and magnetic braking are addressed by Hurley et al. (2002) though are beyond the scope of this study. To see in detail how the BSE models dissipation mechanisms see Hurley et al. (2002).

1.5.2 Roche Lobe Overflow

As described by Hurley et al. (2002), the effective gravitational potential in a frame rotating with a circular binary system forms equipotential surfaces called Roche surfaces. As illustrated by Ostlie and Carroll (2007) very close to either star, the Roche surfaces are nearly spherical in shape, however farther away, the combined influence of each star's gravitational potential on each other distorts their individual Roche Surfaces into teardrop shapes until they finally touch; this point is defined as the *inner Lagrangian, or L_1 point*. As previously noted by Hurley et al. (2000), evolution of a star ultimately leads to decreasing T_{eff} due in part to the swelling of the outer envelope as it ascends the Giant Branch (GB). If either star expands during

evolution as to fill its Roche lobe, then gas can flow from the outer layers of that expanding star passing through the inner Lagrangian point that connects the two Roche lobes and be accreted by the companion star. According to Marinović et al. (2008) mass transfer via RLOF proceeds at a much higher rate than mass transfer from stellar winds which are generated by the radiation pressure of the star and ion flow along stellar magnetic field lines into the ISM (Ostlie and Carroll 2007). In RLOF some or all of this gas may be captured by the companion and therefore in concurrence with the Vogt – Russell theorem, Hurley et al. (2002) concludes that the subsequent evolution of both stars will take a different course from that of isolated or single stars.

1.6 Population Synthesis Codes

As with all theories, understanding of stellar evolution must be tested against observation. One way to do this is to attempt to reproduce the findings of star surveys in star clusters, using population synthesis, the method of choice for this study. In order to make population synthesis statistically meaningful, Hurley et al. (2000) suggests that it is necessary to evolve a large sample of stars. To synthesize n examples of a particular type of star, there exists an associated error in the measurement of $\pm \sqrt{n}$, which means that for rarer stars perhaps millions of possible progenitors are required to obtain a sufficiently accurate sample (Hurley et al. 2002). As Hurley notes, detailed evolution codes and hydrodynamic models (Sills et al. 2001) can take several hours to evolve a model of only one star. It is therefore desirable to generate a large set of those lengthy, detailed models and then present them in some convenient form to more simply utilize the results. This is motivation behind population synthesis algorithms.

One approach to achieve the population synthesis model is to approximate the data produced by the lengthy, detailed models via interpolation schemes which then generate formulae as functions of stellar age, mass, and *metallicity*⁷. Expanding on the work of Eggleton, Fitchett & Tout (1989), Hurley et al. (2000) produced a set of single star evolution (SSE) formulae which were packed into a rapid evolution algorithm. Hurley claims that this rapid, prescription based, evolution scheme can evolve one million stars in the same time required to evolve a single detailed evolution track. Therefore the speed, coupled by the accuracy of the

⁷ In astronomy, any element heavier than He is a metal. Metallicity refers to the fraction of the total mass of elements heavier than He to the total mass of the gas (Ostlie and Carroll 2007).

formulae which Hurley et al (2000) claims exhibits less than 5% error with respect to the detailed models, makes the SSE package ideal for any project which requires information derived from the evolution of a large number of stars.

Hut et al. (1992) reiterates that binary stars represent a significant and important population within a star cluster and are present from the time of formation. Reinforcing the proposition of Stryker (1993), Hurley et al. (2002) suggests that the effects of close binary evolution may explain the existence of stars such as blue stragglers (BSs), which cannot be explained by single-star evolution. While many of the processes involved are not understood in detail, Hurley et al. (2002) advocates that a qualitative picture of how binaries evolve is known. Models for binary evolution have been presented in the past (e.g. Whyte & Eggleton 1985; Pols & Marinus 1994; Portegies Zwart & Verbunt 1996). However, the model used in this study is that of Hurley et al. (2002) which supersedes the work of Tout et al. (1997) by including eccentric orbits and stellar spins that are subject to tidal effects as well as the inclusion of mass accretion from a stellar wind.

The SSE package of Hurley et al. (2000) is fully incorporated within the BSE and provides the underlying stellar evolution of the binary stars as the orbital characteristics are evolved. In fact, the SSE algorithm provides the stellar luminosity, radius, core mass, core radius, and spin frequency, for each of the component stars as they evolve. The prescription for mass loss from stellar winds is also included in the SSE portion of the algorithm (Hurley et al. 2000).

The first step in the evolution algorithm is to initialize the binary. This involves assigning a mass to each star, an orbital separation or equivalently an orbital period, and an eccentricity. The evolution begins with both stars on the ZAMS and a separation such that the binary is *detached*. Other initialization parameters are also allowed, but shall not be considered here.

For the purpose of the algorithm, the evolution of a binary is separated into two distinct phases. The first is called *detached* evolution, which occurs when neither star is filling its Roche lobe. The second phase is referred to as *roche* evolution and occurs if either star is filling its Roche radius. The Roche lobe radius is calculated using the expression given by Eggleton (1983) which depends on the mass-ratio of the stars and the orbital separation. If the radius of a star exceeds its Roche-lobe radius it is deemed to be *filling* its Roche lobe.

Each star has its own evolution time-step, Δt_i which includes restrictions that prevent the star from changing its mass by more than 1%, or its radius by more than 10%. For binary evolution Hurley et al. (2002) explains that sufficiently small time-steps must be chosen so that the radius of the primary does not increase excessively over any single time-step. This aids identification of the time when the star first fills its Roche lobe.

In its most basic form, the algorithm can be seen as moving the binary forward in time within the *detached* phase until one star fills its Roche lobe. At this point, the evolution switches to the *roche* phase which deals with all facets of evolution associated with binary mass transfer. Switching between the *detached* and *roche* phases is permitted, as is following the evolution of a single star in the case two stars coalesce. In either the case a single star is formed due to coalescence of two stars resulting from RLOF or stellar merger resulting from other angular momentum loss mechanisms, the final product continues evolving according to the SSE algorithm with a new mass equal to the sum of its binary progenitors (Hurley et al. 2002).

Details of the calculations and decision-making involved in each step of the algorithm can be found in Hurley, Tout, & Pols (2002). In most cases, Hurley explains that these are based on expressions and theory from the literature. Prescribed outcomes are derived from the most accepted theory or models available. If the theory changes or a new model emerges suggestive of a different outcome, then the algorithm is updated to reflect this. Hurley points out though that parameterized binary evolution naturally involves a number of input parameters that reflect uncertainties in the underlying theory, affecting the evolution and outcomes. As noted by Chen and Han (2009), inappropriate choice for these parameters may inhibit the BS production capabilities of current binary star evolution algorithms.

1.7 Documentation of mass transfer

Since the popular hypothesis for BSs formation is the rejuvenation of hydrogen rich material, mass transfer in a binary from a companion to a MS star provides a mechanism for this to happen (Hurley et al. 2005).

There are six scenarios treated in the BSE that allow for rejuvenation, and or mass transfer, onto a MS star from a companion during the evolution of the binary system. As mentioned previously, if through some mechanism sufficient orbital angular momentum is dissipated, both stars in the binary systems may spiral inwards and merge. Outcomes from such

collisions depend on various impact parameters, which in turn depend on the relative velocity and the relative sizes of the stars involved, as well as their structure. Such details are provided by Hurley et al. (2002) though are not examined here. Alternatively, mass transfer can occur during the aforementioned process of Roche Lobe Overflow (RLOF). Depending upon the evolutionary phase of the star filling its Roche lobe, Hurley et al. (2005) categorizes three chief scenarios in agreement with Kippenhahn, Wiegert & Hoffmeister (1967). Keeping in mind that all forms of mass transfer necessitate the transfer of mass is onto a MS star, *Case A* RLOF indicates that the companion donating mass to the MS star is *another* MS star. As noted by Hurley et al. (2005) this process typically occurs in close period binary stars (on the order of days) and produces BSs also in a very short period system. *Case A* RLOF can also culminate in the coalescence of the system due to the close separation distance between the stars, hence producing single BSs. *Case B* RLOF is characterized by the donating star having evolved to the giant branch. This form of RLOF occurs in slightly wider binaries ranging from tens of days upwards of one hundred days, resulting in a short period circular binary containing a BSs and a White Dwarf (WD) companion (for details concerning stellar types see Hurley et al (2000, 2002)). The last case of RLOF categorized by Hurley et al. (2005) is *Case C* RLOF. Here, BSs in long-period binaries, ranging from approximately 100 to nearly 1000 day periods, may be produced by accretion of material from an Asymptotic Giant Branch star (AGB). In most cases, the BSs produced by *Case C* mass transfer will be circularized, or have an eccentricity of zero⁸. In fact, Hurley et al. (2005) states that the binary orbit will be circular in practically all cases except for wind accretion.

2. Objectives

The objective of this project is to simulate the evolution of a large population of binary stars up to a given age, select any BSs that may have formed, and compare their orbital parameters and CMD locations with observed binary BSs found in open clusters. Ultimately, the results will be used to support or refute the hypothesis that binary star evolution can sufficiently produce the quantity and diversity of the anomalous BSs.

⁸ Recent studies by Marinović et al. (2008) provide contrary evidence that RLOF from an AGB – MS can occur leaving the binary with a non-zero eccentricity owing to a previously untreated enhanced mass loss mechanism.

Two fundamental simulations will be made, the first to an age of 7 *Giga-years* (Gyrs) and a second to 2.4 Gyrs corresponding to the predicted ages of open clusters NGC 188 and NGC 6819, respectively. For both simulations, the quantity of BSs as well as the percentage of BSs in binary will be calculated and compared to the observed quantities found in both NGC 188 and NGC 6819. Moreover, comparisons will be made to observed BSs orbital parameters in NGC 188 as identified by Geller et al (2008, 2009), along with a comparison to the observed CMD location of the BSs. At this time, orbital parameters for those BSs found in NGC 6819 are unknown; however, this does not hinder comparison to the CMD as found by Hole et al. (2009). Finally, a correlation between the specific types of mass transfer leading to the formation of the BSs generated by the simulation will be documented and any notable trends discussed.

The orbital parameters of interest for this study are the *period* (time of one complete revolution) and *eccentricity* (a measure of ellipticity of the orbit shape) for BSs found in binary systems. More precisely, the *distributions* of the period and eccentricities of all observed and simulated BSs in binaries were compared.

3. Method

3.1 Initialization

As previously mentioned, the first step to any simulation is the *initialization* of the parent population of stars. Initialization is the process of assigning the total cluster mass, or equivalently the initial, total number of stars, the *individual* masses of each star in the population, and the orbital period and eccentricity to every primordial binary. To achieve this, the algorithm uses various distributions taken from theory and observation to assign these parameters to all single stars and primordial binary systems at once.

The quantity of stars chosen to initialize is typically chosen according to calculated cluster masses derived directly from observation. Geller et al. (2008) calculated a present virial or total mass of NGC 188 of 2300 ± 460 solar masses, according to an equation provided by Spitzer (1987). Observations by Mathieu (1983, 1985) are suggestive that the masses of M67 and NGC 188 may be similar, and in fact Hurley et al. (2001), derived a *present* total cluster mass of 2500 solar masses for M67 in agreement with the predictions of Mathieu (1983, 1985). Therefore, following closely a model of M67 provided by Hurley et al. (2005) which chose to initialize 12,000 initial binary systems and single stars, the simulations in this study were

initialized with 10,000 binary systems and single stars. Note that 10,000 binary *systems* corresponds to 20,000 stars, therefore the total number of stars in each simulation is 30,000.

The observed period and eccentricity distributions of the *parent* population of binary stars used were those formulated according to observations by Duquennoy & Mayor (1990). Duquennoy & Mayor (1990) made observations of binary field stars and then compared their distribution of orbit eccentricity and period to those of binaries in young open clusters. Interestingly, the parameters of the field binaries matched those of young open clusters. According to Duquennoy & Mayor (1990), this correlation indicates that eccentricities and periods of binaries in young open clusters represent the distributions of the *parent* binary populations. As can be seen in the histograms, the observed parent period distribution (left) can be remarkably approximated by a Gaussian relation with a peak at 4.8 log days (about 63,000 days) and a standard deviation of 2.3. Likewise, the observed parent eccentricity distribution (right) is also approximated by a Gaussian with a mean eccentricity of 0.33 and a standard deviation of 0.156.

Assigning masses is also made via a formulated distribution function. To note, the primary mass distribution used in this study, the one current set as default in the BSE, is taken from the Initial Mass Function (IMF) of Kroupa, Tout & Gilmore (1993), which they derived from stellar distributions toward both Galactic poles as well as the distribution of stars within 5.2 pc of the sun (Hurley et al. 2002).

3.2 Creating statistically meaningful results

In order to make population synthesis statistically meaningful, Hurley et al. (2000), advises that it is necessary to evolve a large sample of stars. A set of simulations were therefore performed, for each cluster age, 7 Gyrs and 2.4 Gyrs for NGC 188 and NGC 6819, respectively. More precisely, 1,000 simulations were performed in succession, the results of which were then tabulated. To distinguish between the results from the constituent runs of the set, the table was demarcated by a number, 1, 2, 3... 1000 identifying each simulation of set. It should be noted that to ensure the results of each run where unique, the BSE must be initialized with a different random seed for each of the 1,000 constituent simulations. The details on the inner-workings of parameter assignment through formulated distributions and the BSE's use of random or

stochastic variables are beyond the scope of this study, and hence are not discussed. In these regards, the BSE was treated as the proverbial “black box.”

3.3 Creating the Synthetic CMD

Among the data output by the BSE, only two pieces of information were needed for construction of the synthetic CMD, specifically the apparent visual magnitudes (m_V) and blue minus visual colors ($B-V$) for each star. This information is automatically tabulated by the BSE, and hence can be read in to a graphing utility. Construction of a CMD was complete when the m_V of all evolved stars from the population, singles, binaries, and BSs alike, were plotted along the ordinate axis and the $B-V$ colors plotted along the abscissa. Identification of BSs is also made by their m_V and $B-V$ color. This selection process is referred to as *photometric selection* and is the method adopted by Geller et al. (2008) to identify BSs on observed CMDs. By setting limits on the luminosities and $B-V$ color indices, photometric selection is performed by overlaying the region where BSs populate the observed CMD, atop the results from the synthetic CMD. Any stars that lie within the defined observed region created by the simulation are then identified as BSs. As seen below, the observed region is defined as being *blueward*, or to the left of, the dashed line in the observed CMD of NGC 188, specifically.

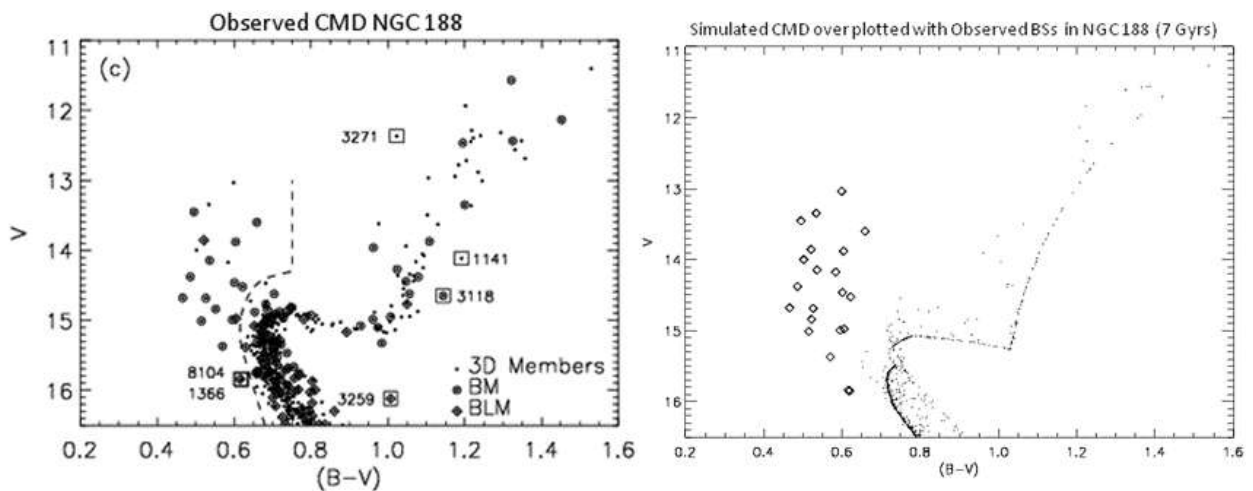


Figure 2

Following the identification of the BSs produced by the BSE across all 1,000 simulations of the set, the next stage is to compile these stars, along with their parameters into a more usable form. An example table is provided below illustrating the photometrically identified BSs

produced from two runs. Note that only BSs that are products of binary star evolution are recorded in this table.

Table 1

3.4 Description of table data

In the BSE algorithm, each star is assigned a number which serves to identify it throughout its evolution, hence the value listed in the column labeled *ID*. *K1* and *K2* indicate the evolutionary phase of a star, for example $k=1$ refers to a MS star with a mass greater than 0.7 solar masses. Because the BSE covers all phases of evolution, *K* values vary from 0 to 15 and any desired details about evolutionary classification phases can be found in Hurley et al. (2000, 2002). Knowledge of specific classes of stars were not directly used in this study, however an important feature of the code is illustrated by them. If the star is in a binary, *K1* refers to the primary star's evolutionary phase, whereas *K2* refers to the secondary or companion star's evolutionary phase. If the star is single, then note that the *K2* value is assigned a value of -1. This is a feature of the code, not an actual stellar type.

Mi0 and *Mi20* refer to the initial masses of the BS primary and secondary stars, at the ZAMS, whereas the *Mif* and *Mi2f* correspond to the final masses of BS primary and secondary stars after the evolution. Again, whenever a -999. is present in the *Mi2f* column, it is implied that the star resulting from the evolution is a single. It should be emphasized that the progenitor may not have been a single star, but could have been a binary which in the process of evolution, merged to form a single star.

The $\text{Log}L$ and $\text{Log}T$ entries represent the base 10 logarithm of the Luminosity and temperature of each star in the simulation. For all simulations, information about the temperature was superfluous and hence not recorded. It is for this reason that one observes a -1 value for the $\text{Log}T$.

$Vmag$ and $BVmag$ correspond to the apparent visual magnitude and B-V or colors of the star(s). These columns were utilized in construction of the *synthetic* CMDs which were then compared to the observational CMDs provided by Geller et al. (2008) and Hole et al. (2009) respectively.

$P0$ and $Ecc0$ correspond to the initial period and initial eccentricity of a binary system that would later evolve to produce BSs. Likewise Pf and $Eccf$ correspond to the final period and eccentricity of the BS if indeed after evolution it remained in a binary. Again, one can observe that in some cases, the Pf is listed as -999. as is its matching $Eccf$ value. As in the previous cases, this value is merely a feature of the code, indicating that the result of evolution of the binary is a single star, thus have no period or eccentricity. It should be noted here that when comparisons between orbital parameters are desired, the general convention is to state the period in units of the base 10 logarithm of period when measured in days (Geller et al. 2008, 2009; Hole et al. 2009). In this way, one can better compare the relationship between eccentricities (which ranges from 0 to 1) to the periods of the binaries (which may extend to thousands of days).

Though unused in this study, an interesting output of the code is the rotational velocities of each star about its axis. This information is given for the primary, $Vrot1$, and the secondary $Vrot2$ respectively. The final piece of information generated by the BSE utilized here, is the documentation of the class of mass transfer which resulted in the formation of the BS. Abbreviated as $Mflag$, the types of mass transfer fall under the six general cases previously described.

3.4 The desired results of the BSE

From the synthetically formed BSs, the average quantity produced per run was found via a count of the stars in the ID column and normalization according to the total number of runs. Percentages of synthetic BSs remaining in binaries following evolution were calculated according to the relative fraction of the stars produced that exhibited *some* periodicity (having a Pf value other than -999.0 which is reserved for single stars) to the total number of BSs

generated. Both the average number per run and the percentage of BSs remaining in binary systems were compared to observed fractions provided by Geller et al. (2008, 2009).

To represent the orbital parameter distributions of synthesized BSs in binary, histograms containing the final period and eccentricity were constructed. Bin sizes for the histograms were chosen to match those inferred from Geller et al. (2008) for which observed distributions were presented. Specifically, the period bin size was incremented according to 1.0 log days and the bin size for the eccentricity was incremented by 0.1. Consequently, the height of the bins in the histograms represents the average number of BSs produced whose period or eccentricity was found to lie within the value specified by the bin. Error bars representing the standard fluctuation of that mean were then added.

The simulated orbital parameter distributions were then compared to the observed distributions. As a normalization measure, periods and eccentricities were obtained from Geller et al. (2009) for each binary BSs found in NGC 188, and corresponding histograms were produced using the same bin size and axis incrementation as those generated from the simulation. In this way, a higher degree of precision can be achieved when determining the extent of similarity between the simulated and observed orbital parameters.

A plot of eccentricity versus the base ten logarithm of the binary period (henceforth $e \log p$ plot) was then constructed for synthetic BSs selected from all 1,000 runs in the set, the motivation behind which will be elucidated in results section of this paper. These BSs stars were color coded according to the type of mass transfer which the BSE indicated was responsible for their existence on the CMD. Furthermore, the type of mass transfer forming each BSs in the CMD was tallied and relative percentages per mass transfer type computed for each of the two simulations.

Next, a CMD was constructed onto which the synthetic BSs were plotted. These BSs were given color, also according to the type of mass transfer that formed them. In order to observe any regionalization of stars on the CMD corresponding to a specific form of mass transfer, which was later found to be the case, a series of six CMDs were arrayed illustrating only BSs formed by each of the six respective types of mass transfer as documented by the BSE.

As it will be later illustrated, it was found that for simulated BSs, the mass transfer type is a consequence of the orbital period of the parent binary. Furthermore, it was found that for some types of mass transfer, a correlation existed between CMD location of the synthetic stars and

their mass transfer type. This implies that the period of BSs in binary undergoing select forms of mass transfer is related to location on the CMD. In order to determine whether such a relationship may exist on the observed CMD, the BSs identified by Geller et al. (2008, 2009) were also given color according to their *periods*. As another normalization measure, the observed CMD locations for the NGC 188 BSs were plotted overtop a synthetic CMD. This diminishes the disparity in the scaling between a synthetic CMD, and that of observation. If the predictions of the BSE are true, then the same grouping prevalent on the synthetic CMD according to *mass* transfer type should be mimicked in the observed CMD when color coded according to the periods of the BSs.

3.5 Repeating the procedure for a younger cluster

Following the evolution of a population of stars to 7 Gyrs, in accords with that the age for NGC 188 (Geller et al. 2008), another simulation was performed though to 2.4 Gyrs, representative of the age of NGC 6819 (Hole et al. 2009). As previously mentioned, the number of stars in the parent population to be evolved is an important quantity, (Hurley et al. 2005). For NGC 188, Geller et al. (2008) found 1046 to be classified as cluster members, and derived a virial mass of the cluster of 2300 ± 460 solar masses. From this information a parent binary population of 10,000 single stars and 10,000 binary *systems* were chosen for the evolution. In NGC 6819, Hole et al. (2009) found 1207 stars classified as being cluster members. As noted by Hurley et al. (2005) it is expected that as a cluster ages, its overall mass will decline. Though a calculation was not performed, it was assumed that beginning the 2.4 Gyr simulation with an identical parent population of stars would be sufficient to gain at least an idea of the number of BSs expected, the binary frequency, as well as the CMD locations of synthetically formed BSs. In addition, the parent population was initialized with the suggested metallicity of NGC 6819 according to Hole et al. (2009). All other parameters were chosen according to the recommended default settings of the BSE.

In addition to comparing the number of BSs and the binary frequencies, to gain a normalized view of the CMD locations of the observed BSs in NGC 6819 to those generated by the simulation, the *mV* and *B-V* colors of the observed BSs presented by Hole et al. (2009) were superimposed on a simulated CMD and compared in the same way as that described for the NGC 188 CMD. Finally, the BSs were color coded according to those that are in binary. Note,

because the orbital periods of the NGC 6819 BSs are currently unknown, the color applied to the NGC 6819 CMD has no basis for a particular formation pathway, but does served to point out the CMD location of the binaries.

4. Results

4.1 Simulated quantities of BSs

Hurely et al. (2008,2009) identifies 21 candidate BSs within NGC 188, of which 16 are classified as binary. Geller et al. (2008) expresses that this 75% binary BSs frequency is high when considering that all of them are in detached states. Following 7 Gyrs of evolution of the parent population of stars, after averaging the quantity of BSs per run, it was found that only 4-5⁹ BSs were produced per simulation, in stark disagreement with the quantity of BSs found by Geller et al. (2008). The binary fraction for the 7 Gyr simulation was found to be 57%, which is 18% less than observation.

Hole et al. (2009) identifies 12 candidate BSs within NGC 6819. Of note, only 4 of the 12 BSs in NGC 6819 are found to be in binary star systems, hence exhibiting only a 33% binary fraction. This contradicts the larger 75% binary BSs frequency found by Geller et al. (2008, 2009) in NGC 188. To this, the average number of BSs produced by the 2.4 Gyr population was 5 BSs. A binary frequency of 48% in the younger cluster was slightly smaller than produced by the 7 Gyr evolution.

4.2 Simulated orbital parameters

The following collection of plots juxtaposes the observed period and eccentricity distributions from the binary BSs observed in NGC – 188 according to Geller et al. (2009), to the averaged eccentricity and period distributions of the binary BSs photometrically selected from 1,000 simulations. Beginning with right column, which displays the eccentricity distributions, the large number of stars which have been tidally circularized during evolution is reflected in both observation and simulation. It is found that in observation, a larger fraction of observed BSs have eccentricities between 0.1 and 0.3, than in the simulated BSs. However fewer observed BSs have periods beyond 0.3 than in the simulated BSs.

⁹ 4 – 5 BSs represents a lower limit of BSs generated per run. If one extends the region on the CMD to a broader range of magnitudes and colors, then we obtained on average 10 – 11 BSs at a 77% binary frequency.

The most salient find is the similarity between the observed and simulated period distributions. The results of the simulation are in agreement with observation of a large number of BSs having periods near 1,000 days. Upon closer inspection, one should note that the bin is shifted slightly to longer period in the simulation than in the observed NGC 188 BSs. Though there exists a vast disparity in the overall quantity of BSs produced from the simulation, it is important to note that those that *were* created fall within an analogous period range.

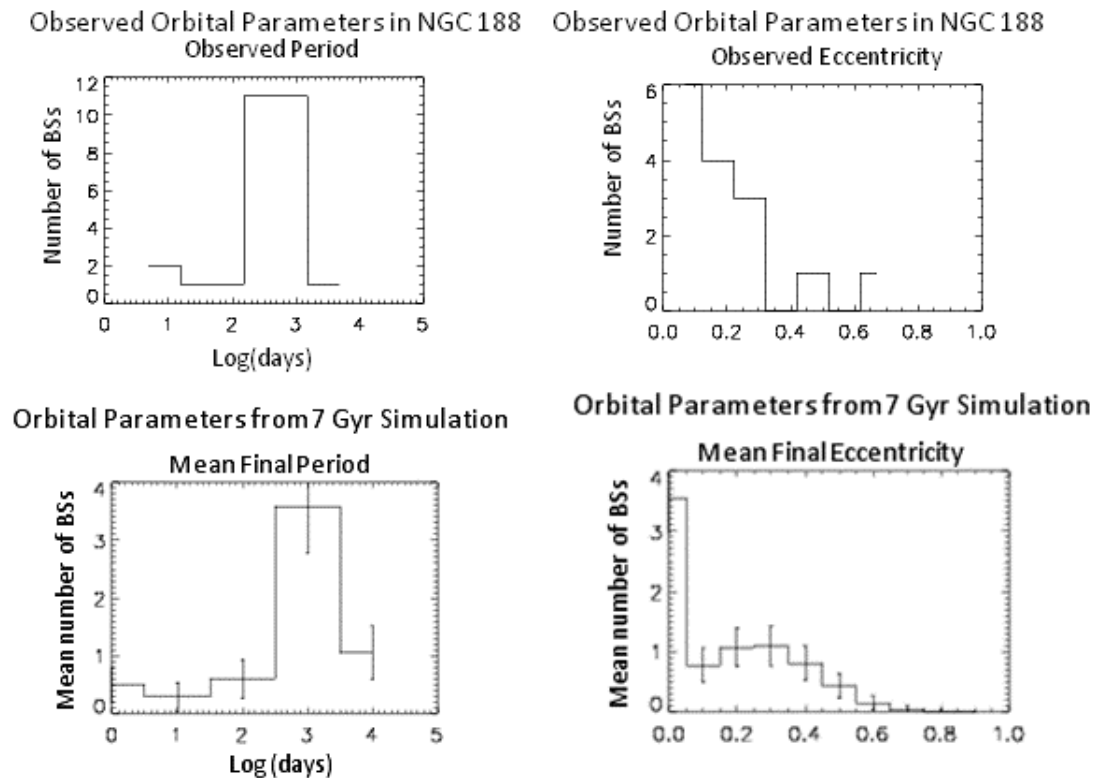


Figure 3

Since current orbital periods and eccentricities have yet to be determined for those BSs in NGC 6819, only the orbital parameters for the NGC 188 BSs could be directly compared to simulation. Nevertheless, orbital histograms representing the averaged periods and eccentricities of the 2.4 Gyr simulation were also compared to the results of the 7 Gyr simulation. The similar shape of the eccentricity histograms is a consequence of the parent eccentricity distribution that were used to initialize the population (Duquennoy & Mayor 1990). The similarity in the period histograms indicates that even at an age of 4.6 Gyrs younger, effectively the same range of

periods exist for BSs present in the population. Over the age range from 2.4 Gyrs and 7.0 Gyrs, then it might be proposed that BSs period distributions are approximately constant.

Orbital Parameters from 2.4 Gyr Simulation Orbital Parameters from 7 Gyr Simulation

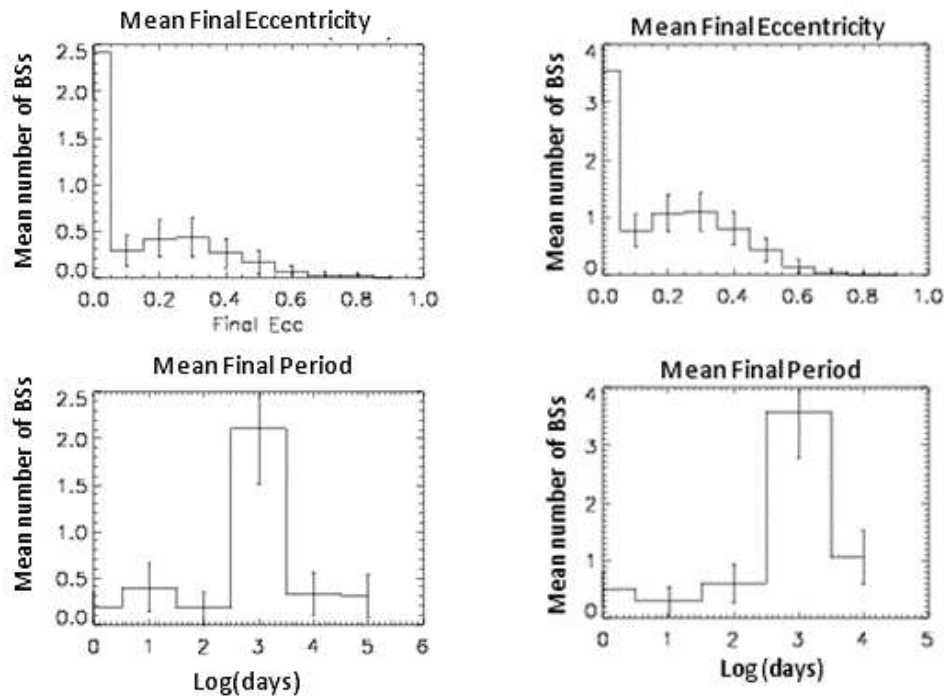


Figure 4

4.3 Relating eccentricity, period, and mass transfer type

In order to determine any relationships that may exist between the eccentricity and period, it is customary to plot an $e \log p$ plot such as that provided by Hurley et al. (2008). The plot below illustrates that of those stars populating the representative 1,000 day period bin in the observed histograms, these binaries are found in a variety of eccentricities. This same trend was also observed in the simulated 7 Gyr cluster.

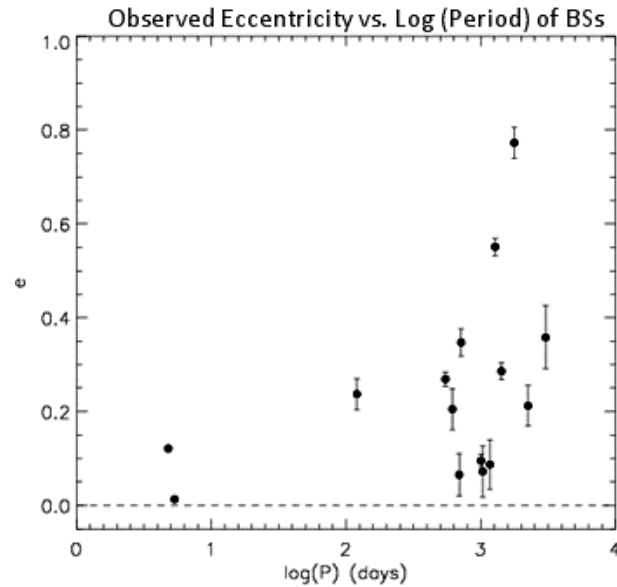


Figure 5

The plots below depicts the synthetically formed BSs compiled from 1,000 simulations. The colors indicate the type of mass transfer responsible for the existence of the BSs as modeled by the BSE. Immediately, one can observe that the colors are arranged in vertical columns according to pre-defined ranges in *period*. This implies that the mass transfer type in a binary system is a function of the period of the binary orbit. Thus, according to the BSE, knowing the period of BSs binary system is tantamount to knowing the type of mass transfer responsible for the formation of the BSs. Moreover, it is seen that effectively all *Mergers* and *RLOF* formation pathways produced BSs in tidally circularized binaries. This last result is in accords with the simulations of Hurley et al. (2005).

The bottom row of plots illustrates the resulting eccentricities and periods for binary BSs polled at the end of all 1,000 simulations. After evolving the two models for 7 Gyrs, and 2.4 Gyrs respectively, it was found that beyond a period of approximately 1,000 days, the BSs begin to have non-zero eccentricity values. The BSE recorded the responsible mechanism in both simulations to be wind accretion. In the simulation to an age of 7 Gyrs, the donating star was a Red Giant Branch Star. In the simulation to 2.4 Gyrs, the donating star was a more massive Super Giant star. It should be commented on here that the BSE also includes the possibility of Hertzsprung Gap star (HG) and Subgiant star winds within the classification naively and somewhat inaccurately referred to as Red Giant Branch star wind throughout this paper. For

more details on the evolutionary stages of stars treated in the BSE, see Hurley et al. (2000; 2002).

In comparison to the observed $e \log p$ plot provided by Geller et al. (2008), it is suggested here that the prevalent quantity of stars exhibiting non-zero eccentricity in both cases is indicative of an existing relationship. If so, the results of the simulation may predict that the NGC 188 BSs observed in this period range with non-zero eccentricity, were formed through wind accretion from a Giant Branch star as opposed to merger or Roche Lobe Overflow. Stated more restrictively, following 7 Gyr of evolution governed exclusively by binary star evolution, then some of the BSs found in binaries with an eccentricity other than zero having periods near 1,000 days may be the products of mass transfer from stellar wind accretion.

Considering now the outcome of the 2.4 Gyr simulation, a nearly parallel result is found. Concentrating only the group of BSs having non-zero eccentricities following 2.4 Gyrs of evolution, the one point of disparity is the *type* of wind responsible for the production of the BSs. In the younger cluster, no Red Giant Branch star wind is observed. On the other hand, Super Giant star wind is. Inferring from the previous discussion put forth by Ostlie and Carroll (2007) and in accords with Hurley et al. (2000; 2002), because Super Giant stars contain greater mass, then it is expected that their evolution will proceed more rapidly than a less massive Red Giant Branch star. For this reason, the lack of Red Giant winds in NGC 6819 reflects the younger age of the cluster. To interpret the colors on the $e \log p$ plot and all that follow, the following legend will be useful:







	Case M	Merger
	Case A	Roche lobe over in two MS stars
	Case B	Roche lobe overflow in a MS star and a Giant star
	Case C	Roche lobe overflow in a MS star and an AGB star
	Case BW	Wind Accretion from a Red Giant star
	Case CW	Wind Accretion from a Super Giant star

Table 2

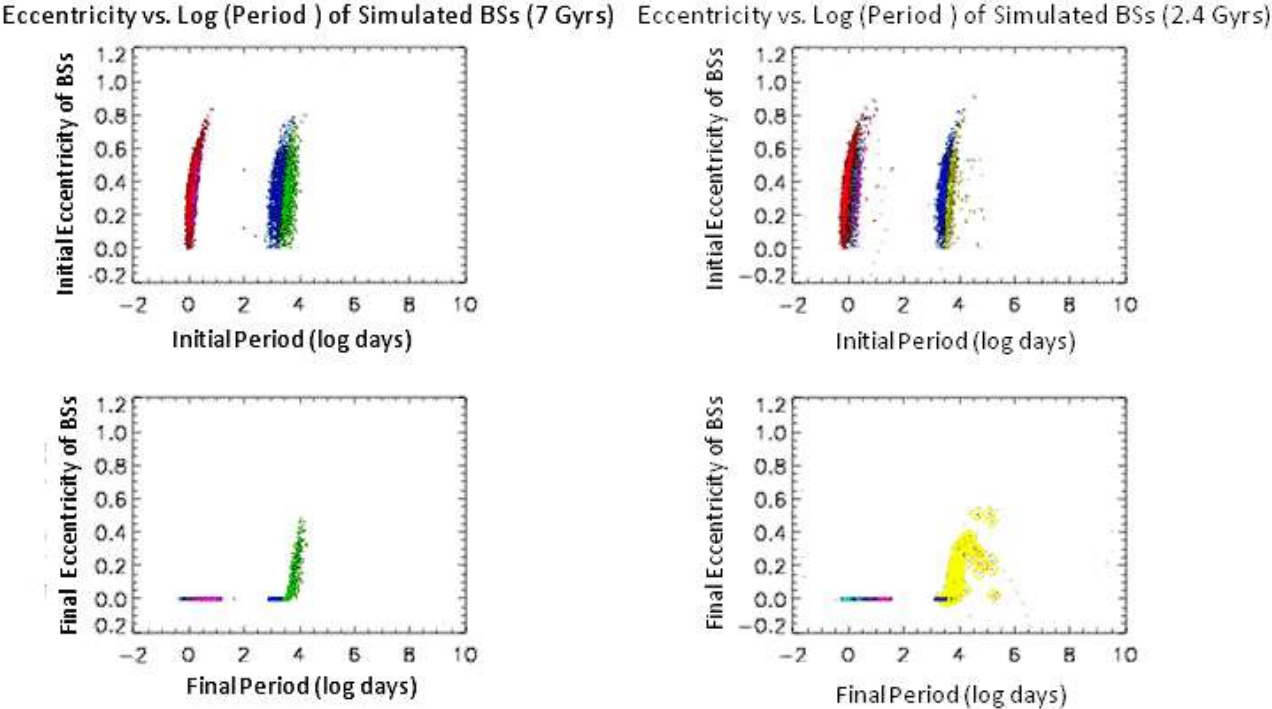


Figure 6

The following charts illustrate the relative percentage of each type of mass transfer responsible for the production of the BSs in the simulation. As mentioned above, the most noted feature is the effective absence of mass transfer from wind accretion of a Red Giant star in the 2.4 Gyr evolution, and its presence in the 7 Gyr evolution. Wind accretion from a Super-Giant was found to produce about 17% of BSs, or roughly one out of the five BSs produced by the BSE. In the 7 Gyr simulation, it was found that 22% of the BSs produced per run was via Red Giant wind corresponded likewise to about 1 BS per simulation.

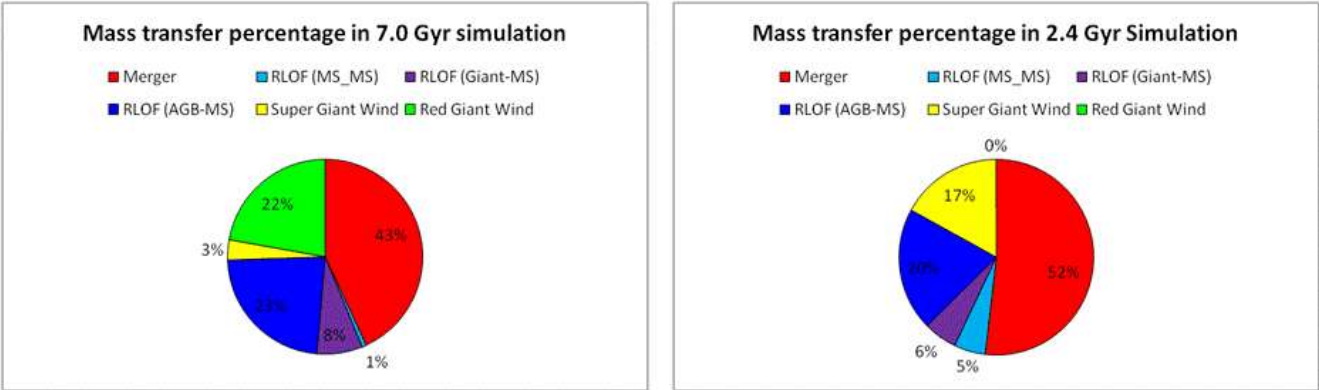


Figure 7

4.4 CMD location of simulated BSs according to mass transfer type

The following series of six CMDs were arrayed such that any preferential location of the BSs on the CMD with respect to mass transfer type could be exposed. What is seen in each plot is a unique color, representative of a unique form of mass transfer for the 7 Gyr simulation. While mass transfer via mergers and RLOF via MS – MS or MS – Giant Branch star exchange exhibits no apparent regionalization, it is found that RLOF from an AGB – MS star, along with wind accretion from either Super Giant or Red Giant Branch star is highly regionalized very near the MS turnoff of the cluster.

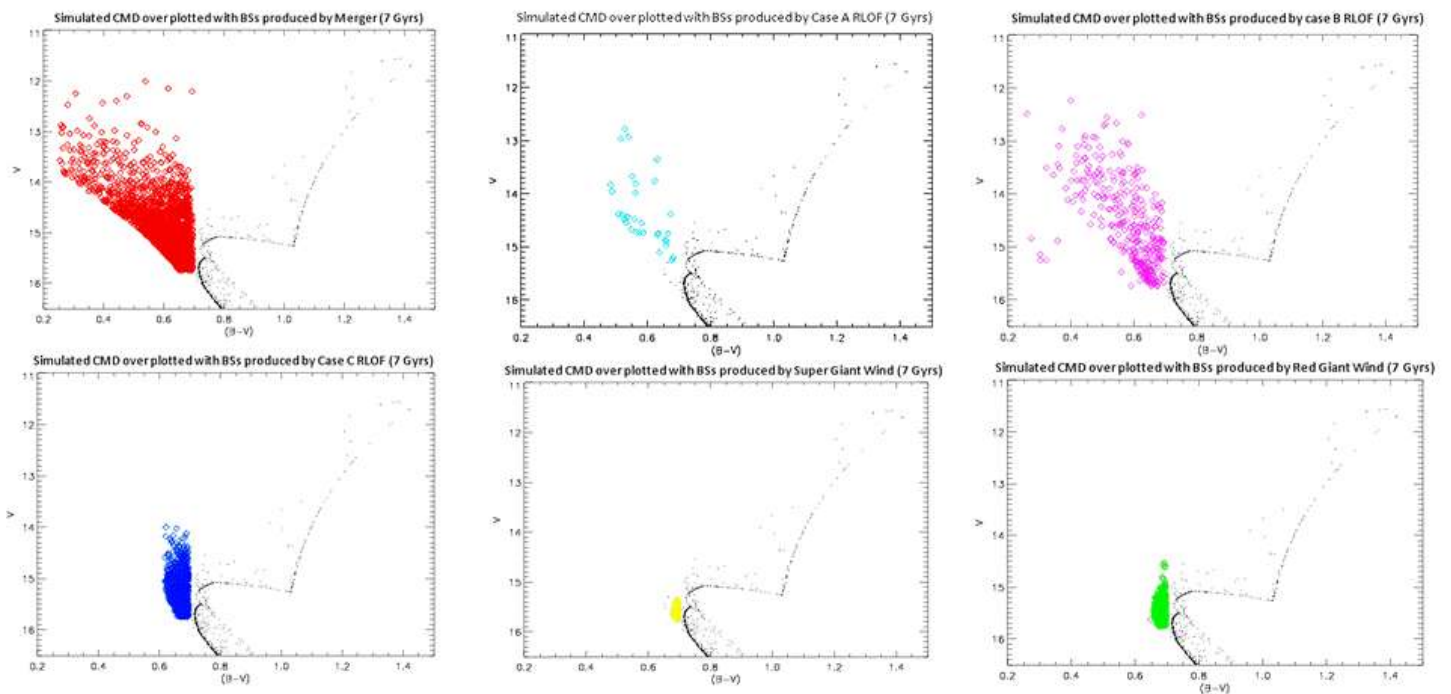


Figure 8

A similar array of color coded CMDs were generated for the 2.4 Gyr simulation as to determine whether the 4.6 Gyr age discrepancy between the simulations had any noticeable effect on the regionalization of mass transfer type to the luminosity and temperature of the BSs. It was found that like the 7 Gyr simulation, no preferential CMD location was applicable to mass transfer from BSs formed by mergers and MS – MS or MS – Giant Branch star RLOF. What was found however is that the *degree* of regionalization for MS – AGB RLOF and Super Giant wind accretion especially, has broader, less defined locations. This implies that at younger age,

the formed BSs are hotter, and hence bluer, and also brighter. The relative abundance of stars formed via Super Giant winds in the 2.4 Gyr simulation with respect to those generated likewise in the 7 Gyr simulation is clearly observed. Similarly, the dearth of Red Giant Branch wind accretion can be seen in the 2.4 Gyr simulation with respect to the 7 Gyr simulation. According to the previous discussion, these facts are consistent with disparity in the ages of the simulation.

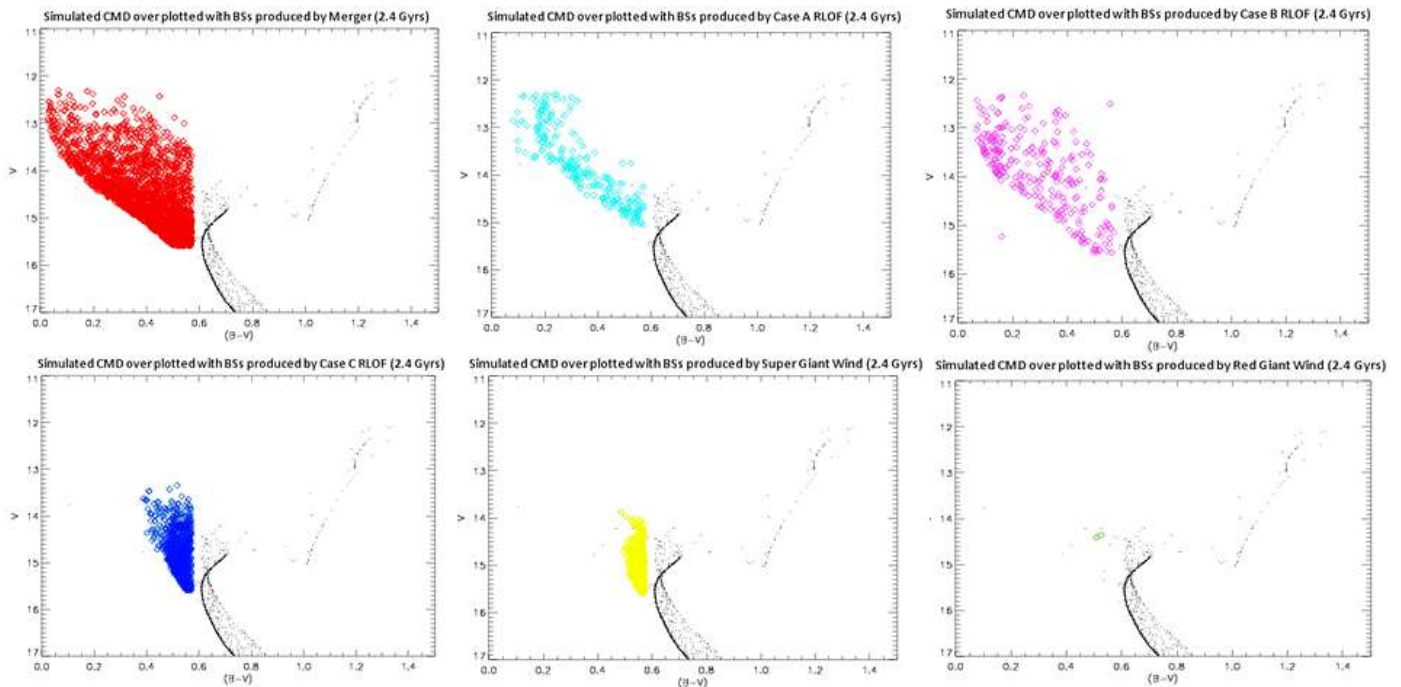


Figure 9

4.5 Predicting NGC 188 BS formation from simulated period trends

In following diagram the right plot represent the 7 Gyr simulated CMD. The stars enclosed by the diamonds represent the mV and $B-V$ colors of the *actual* BSs observed in NGC 188 (Geller et al 2008, 2009). Note that a selection of the *observed* BSs is color coded. In NGC 188 (left) those stars highlighted in green have periods greater than approximately 3.3 log days which corresponds to mass transfer via wind accretion by a giant star onto a MS companion, as inferred from the simulated $\log p$ plot above. The regionalization of the BSs produced via Red Giant winds in the 7 Gyr simulation are markedly closer to main sequence turnoff than are those observed in NGC 188. Inferring from the previous discussion provided by Ostlie and Carroll (2007), the simulated BSs formed by Red Giant wind are therefore cooler than those BSs found in NGC 188. Thus, even though the highlighted NGC 188 BSs have periods indicative of

formation via Red Giant winds according to the BSE, it appears that this mechanism cannot produce BSs hot enough to accurately reconstruct the entire observed CMD.

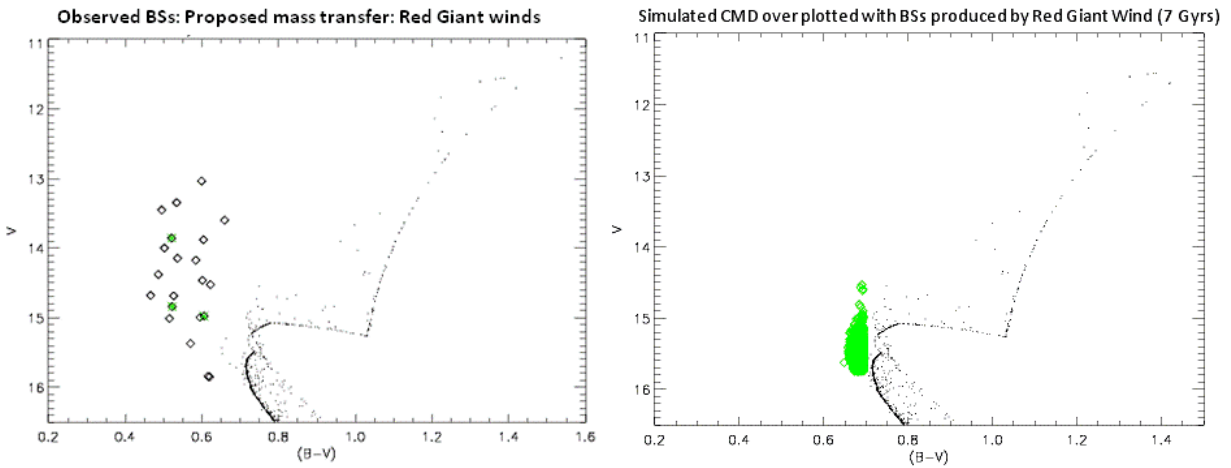


Figure 10

In light of the quantity of BSs found to be produced per run attributable to stellar winds being about 1 BSs in either the 7 Gyr or the 2.4 Gyr clusters, then the immediate conclusion is that wind accretion alone does not present itself a likely mechanism to produce all of the BSs populating the 1,000 day period range in either NGC 188 or NGC 6819. It is very likely however that the mechanism could have resulted in the formation of a few of the stars, however based on the finds of this study, to make the claim that mass transfer from wind accretion can account for the *number* of stars observed having a similar period range is unwarranted.

As an extra measure, the single stars in NGC 188 were selected and assigned a color of red corresponding to mass transfer by merger, and compared with the BSs formed by merger from simulation. Then, those BSs having periods larger than 0.5 log days but less than 2.0 log days were assigned a color of purple according to mass transfer via Giant star – MS RLOF. Finally, those observed BSs having periods in the range between 2.0 log days and 3.3 log days were assigned the color of blue according to mass transfer from an AGB – MS star through RLOF. These period ranges were inferred from the results of the $e \log p$ plot shown previously. The results are shown below.

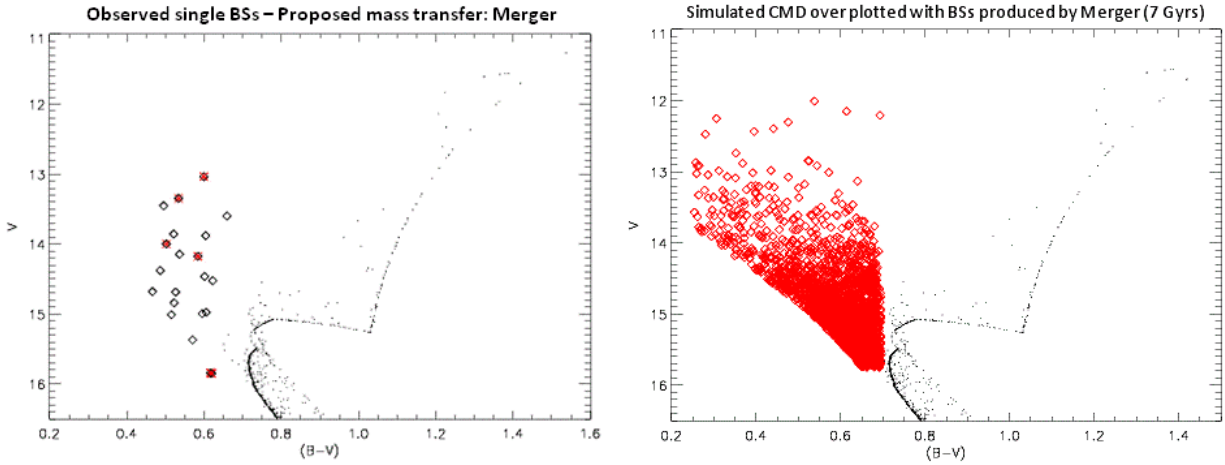


Figure 11

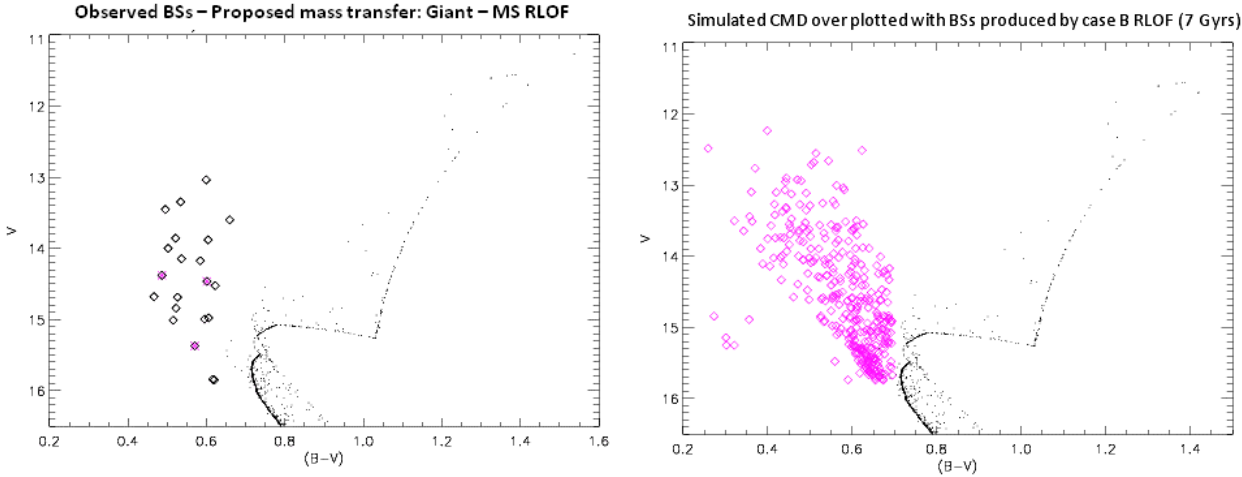


Figure 12

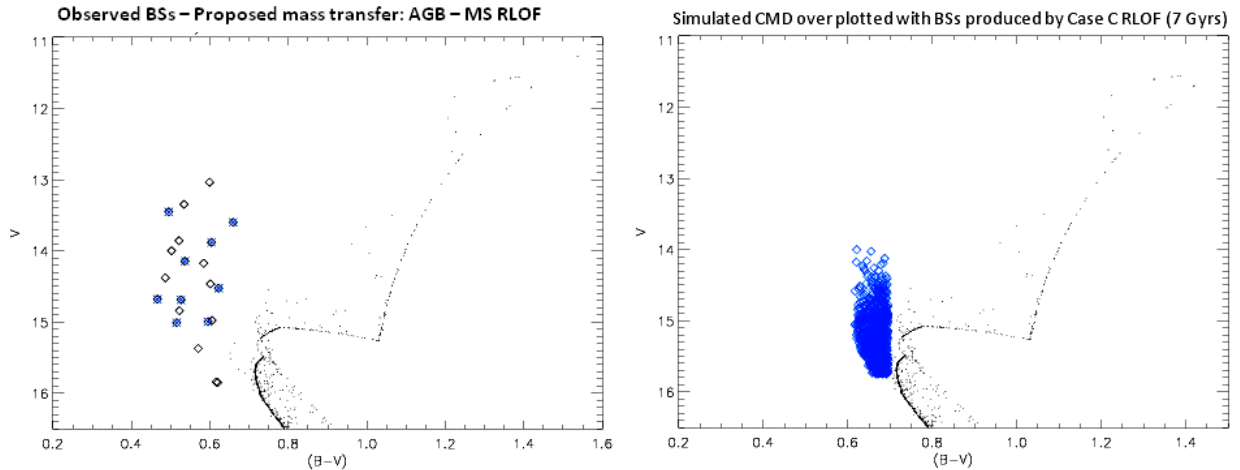


Figure 13

It should be noted that no MS – MS RLOF nor mass transfer by Super Giant winds were selected as proposed formation pathways for the observed BSs because of their relatively low contributions to the BSs produced from the 7 Gyr simulation. Note that the CMD region for stars produced by AGB – MS RLOF in simulation is again more regionalized closer to the MS turnoff than the predicted region of stars on the observed CMD, having periods indicative of mass transfer by this mechanism. On the other hand, there is no apparent disagreement in the CMD locations for the BSs whose periods correspond to mass transfer by Giant Branch star – MS RLOF or merger through angular momentum loss. It is observed that BSs predicted to have formed by merger populate a region on the CMD of lower mV (or higher luminosity) than those predicted to have been formed by Giant – MS RLOF.

Following color assignment to the NGC 188 BSs, the percentages of stars inhabiting each period interval were calculated and compared to the respective percentages computed from the synthetically evolved BSs according to mass transfer type.

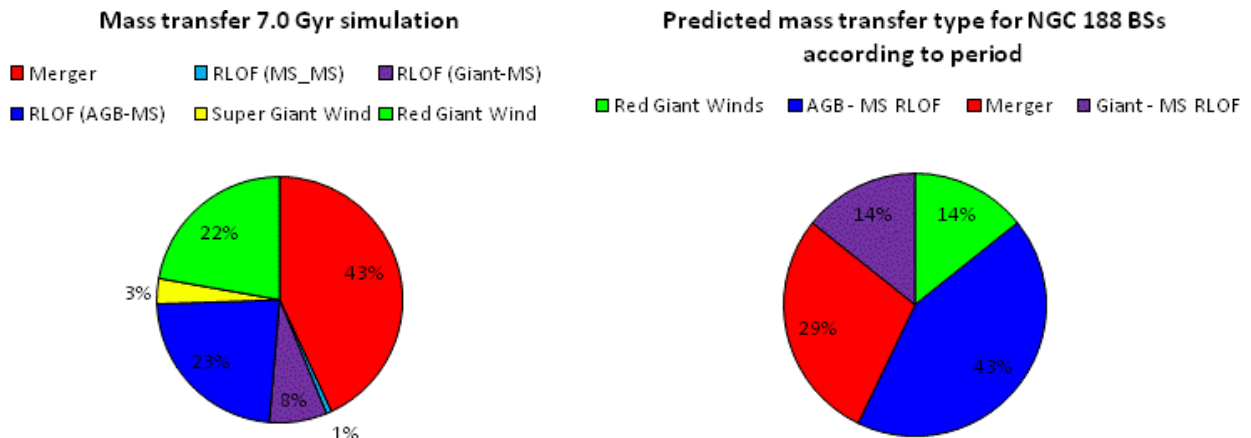


Figure 14

Whereas the largest fraction of synthetic BSs were formed through merger, to note 43%, the most prevalent formation predicted from the periods of the observed BSs was RLOF from an AGB star onto a MS star, coincidentally at 43%. Conspicuously, the percentage of stars formed through wind accretion in the simulation at 22% was comparable to the number of stars in NGC 188 identified within the relevant period interval corresponding to Red Giant Branch star winds at 14%. Similarly the disparity between the 8% production from Giant – MS star RLOF from simulation to the 14% predicted from the observed BSs proves also to be comparable.

5. Discussion

5.1 Comparing lack of BS production with other authors

It is evident from this study that the major point of inconsistency between observed BSs and simulated BSs for both NGC 188 and NGC 6819 is the quantity that the BSE is capable of producing. Following this, is the disagreement in the CMD locations of observed BSs when selected according to the period of the binary. What is noteworthy is that other binary star evolution algorithms have also experienced similar points of incongruity. Chen and Han (2009) employed a similar binary population synthesis code originally developed by Han et al. (1994) to investigate the BS formation from a primordial binary population, or via binary star evolution. Chen and Han (2009) have also modeled NGC 188 according to Han et al. (1994) population synthesis code, and found the BSs production from angular momentum loss, or what is referred to a merger in the BSE, produced approximately 4 BSs, whereas the processes of primordial binary evolution, that is to say the processes of RLOF, could only produce approximately one

BSs. In all, the Chen and Han (2009) simulation of NGC 188 produced approximately 5 BSs in agreement with the number found in this study using the BSE of Hurley et al. (2002).

5.2 Regionalization of simulated AGB – MS RLOF BSs

Considering the CMD locations of the Chen and Han BSs, Chen and Han (2009) found that several observed BSs in NGC 188 to be bluer than those found from simulation. Chen and Han (2009) propose that enhancement of surface Helium (He) may lead these BSs to appear bluer than those produced from their simulations. Furthermore, they suggest that AGB stars can provide material with high He abundances for clusters older than about 2.24 Gyrs. Chen and Han (2009) conclude that these BSs may have originated from mass transfer between AGB and MS stars and have long orbital periods in old open clusters. What is remarkable is that this proposition by Chen and Han is exactly the mass transfer mechanism predicted by the BSE to account for 43% of observed NGC 188 BSs which constitutes the largest fraction.

5.3 Disparity in simulated BSs formed by AGB – MS RLOF showing $e = 0$.

Another point of concern revealed from this study is that effectively all of the BSs produced via AGB – MS star RLOF in the BSE exhibited an eccentricity of zero. The observed $e \log p$ plot of Geller et al. (2008), in contrast, suggests that BSs within the period interval which the BSE predicts should have been formed via AGB – MS RLOF have non-zero eccentricities. According to Marinović, Glebbeek, and Pols (2008), many binary systems in which the primary star is beyond the AGB evolutionary phase also show significant orbital eccentricities. This signals that there exists some mechanism to counteract the circularizing effects of tidal interaction (Marinović et al. 2008) not treated in the BSE. Marinović et al. (2008) proposed a model for enhanced mass loss from the AGB star due to tidal interaction with its companion, allowing a smoother transition between the wind and RLOF mass loss regimes, currently treated. It was found that in many cases, due to the enhanced mass loss rate of the AGB component at orbital phases closer to the periastron, the net eccentricity growth rate in one orbit is comparable to the rate of tidal circularization. The mechanism was also applied directly to successfully reproduce the orbital period and eccentricity of the Sirius system, which is expected to be circularized under the standard assumptions of binary star interactions (Marinović et al. 2008). Consequently, according to the results of the BSE, formation pathways of the NGC 188 BSs with

non zero eccentricities appear to be explainable by both mechanisms of wind accretion as well as AGB – MS RLOF.

5.4 Possible experiment to test for Observed BS formation via AGB – MS RLOF

Ostlie and Carroll (2007) note that the effective temperatures of AGB stars are quite cool at around 3000K – the sun in comparison has an effective temperature of 5777K. As a result dust grains form in the expelled material. Since silicate grains tend to form in an environment rich in oxygen and graphite grains in a carbon-rich environment, the composition of the ISM between cluster members may be related to the relative numbers of carbon and oxygen rich AGB stars present (Ostlie and Carroll 2007). Furthermore, Ostlie and Carroll (2007) note that of particular interest in the atmospheres of evolved AGB stars, is the presence of the element Technetium (Tc), an element with no stable isotopes. Since $^{99}_{43}\text{Tc}$ is the most abundant isotope found in the atmospheres of evolved AGB stars, then its identification from analysis of the spectra of the selected NGC 188 BSs above as having periods indicative of formation through AGB – MS RLOF, would provide support for predictions made from this study.

5.5 Possible causes for the lack of BSs and final remarks

Chen and Han (2009) suggest that a possible culprit behind the lack of BSs produced from population synthesis codes in general lies in the initialization distributions, particularly of the initial mass functions. For instance, the initial mass function remains an area of open concern and recent studies by Pols et al (2008) show that the IMF may vary between clusters located in the disk of the galaxy and those located in the halo.

Perhaps the most favored explanation is that the low numbers of stars produced by both models indicates that other formation pathways exist for making BSs. Chen and Han (2009) propose that a more recent era of star formation may be the source. Another preferred mechanism of BS formation is by the evolution of the *cluster* which has provoked stellar collisions between both single stars and binary systems in N-Body encounters, (Stryker 1993; Hurley et al. 2001, 2002, 2005; Chen and Han (2009)).

It should be noted that binary star evolution has been well studied over the past 50 years, and has been successful at describing other anomalous stars such as Algols, Symbiotic stars, cataclysmic variables, and type Ia supernovae (Chen and Han 2009). It is proposed that

primordial binary evolution mechanisms is the most likely source of BSs, especially in low density open clusters, considering the mounting observational evidence of the existence of binaries in these and all systems (Stryker 1993). Nevertheless, even in lieu of 50 years of progress, BSs still remain a challenge to explain.

6. Summary & Acknowledgments

A systematic study of BS generation from synthetic evolution of a population of primordial binaries (population synthesis) was performed using the Binary Star Evolution algorithm of Hurley et al. (2002). Two simulations were made, the first population was evolved to 7.0 Gyrs corresponding to the proposed age of NGC 188 (Geller et al. 2008) and the second simulation to an age of 2.4 Gyrs according to the age of NGC 6819 (Hole et al. 2009). Each simulation was comprised of a set of 1,000 individual simulations as to provide a sufficiently large sample from which statistically meaningful results could be calculated. Following photometric selection, the average number of BSs from both clusters as well as the binary percentage were calculated and compared to observation (Geller et al. 2008, 2009; Hole et al. 2009). The averaged eccentricity and period distributions of the synthetically produced BSs were then compared only to those of NGC 188 since currently the period and eccentricities of NGC 6819 BSs are unknown. A relationship between eccentricity, and period was then determined via a plot of eccentricity vs. the base 10 logarithm of the period ($e \log p$) for all stars produced from the set of 1000 evolutions. To this plot, each star was given color according to the type of mass transfer which the model indicated had formed it. The CMD locations of the synthetically evolved populations were then determined for each type of mass transfer that produced the BSs. Based on the results of the simulation that mass transfer type is related to the period of the binary, predictions were made concerning formation pathways of certain NGC 188 BSs.

It was found that the BSE produced on average between 4 – 5 BSs with a binary percentage of 57 %, which is notably in stark contrast to the 21 BSs observed in NGC 188 at a 75% binary fraction (Geller et al. 2008, 2009). The BSE produced a similar quantity in the 2.4 Gyr simulation at approximately 5 BSs with binary percentage of 48%. It was observed by Hole et al. (2009) that 12 candidate BSs exist with a 33% binary frequency. In both cases, the BSE was unable to produce the amount of the BSs observed.

Though the averaged, simulated eccentricity distributions shown less stars in the $0.1 \leq e \leq 0.3$ range, the simulation agreed with observation that a large fraction of BSs are tidally circularized. While there existed a slight shift of the period peak to values less than 1,000 days in the observed period histogram of NGC 188, the overall shape of the simulated BSs remarkably agreed with that of observation. According to the BSE, it was found that mass transfer type is a function of period of the parent binary, and that by knowing the period of the final BS, then a prediction can be made on the type of mass transfer that produced it. Between a period range of 2.0 to 3.3 log days (approximately 100 to 2000 days) Geller et al. (2009) finds 9/21 or 43% BSs in NGC 188. Results from the BSE indicate that this period range corresponds to mass transfer by AGB – MS star wind. Unfortunately, the percentage of BSs formed by AGB – MS RLOF from the simulation is 23% whereas 43% of the BS are found within the specified period interval of the simulation.

Observed BSs tend to have bluer color and lower mV magnitudes than are producible by the BSE, however Chen and Han (2009) propose that in the case of AGB – MS RLOF Helium enhancement may produce bluer BSs than current simulations predict.

Only stars formed by wind accretion were found to produce binary BSs in non-zero eccentricities, and wind accretion appears to occur only at periods longer than approximately 3.3 log days. In contrast, Geller et al. (2008, 2009) finds many BSs in a shorter period ranges than 3.3 log days that have non-zero eccentricity, corresponding to mass transfer by AGB – MS RLOF in the simulation. Marinović et al. (2008) note that AGB – MS star mass transfer has been observed to produce non – zero eccentricity orbits and have proposed a new prescription for mass loss in a AGB – MS system capable of generating non-zero eccentricities which is in accords with the observation of Geller et al. 2008, when coupled with the period range predicted by the BSE.

To test the new prediction that AGB – MS RLOF may be responsible for the formation of some of the NGC 188 BSs with non-zero eccentricity and having periods between 2.0 and 3.3 log days, Ostlie and Carroll (2007) note that spectral traces of Technetium may be used to identify evolved AGB stars, hence spectral signatures of Technetium in the NGC 188 BSs may support the above predictions. The results of this study confirm that BS existence remains a mystery, though perhaps a small addition to unraveling the mystery may have been uncovered in a new formation pathway for observed BSs.

This author would like to express his deepest gratitude to Dr. Robert Mathieu and Aaron Geller, who have made it possible to continue research on the NGC 188 BS population, and for their instruction and wisdom during the summer 2008 REU¹⁰ through which first exposure to this exciting topic was made. A very special thanks is extended to Dr. Jarrod Hurley who allowed the use of the BSE for this study and for answering the many questions posed over the course of the study. I would like to thank Dr. Peter Frinchaboy for allowing the use of his computer on which all of the simulation were ran, and to Stephan Jansen for maintaining network connectivity throughout the term. Another thanks is extended to my advisor Dr. Tracy Hodge aided in analyzing the data and keeping the progress of the research going smoothly throughout the semester.

¹⁰ The summer 2008 REU was funded by the National Science Foundation and the Department of Defense's ASSURE, program through NSF Award AST-0453442.

REFERENCES

- Bondi H., Hoyle F., 1944, MNRAS, 104, 273
- Collier, A., and Jenkins, C. 1984, MNRAS, 211, 391
- Cudworth, K. M. 1985, AJ, 90, 65
- Duquennoy A., Mayor M., 1991, A & A, 248, 485
- Eggleton P. P., 1983, ApJ, 268, 368
- Eggleton P. P., Fitchett M., Tout C. A., 1989, ApJ, 347, 998
- Geller A.M., Mathieu R.D., Harris H.C., McClure R.D., 2008, AJ, 135, 2264
- Geller A.M., Mathieu R.D., Harris H.C., McClure R.D., 2009, AJ, 137, 3760
- Han Z., Podsiadlowski Ph., Eggleton P.P., 1994, MNRAS, 270, 121
- Hole, T.K., Geller A. M., Mathieu R.D., Platais I., Meibom S., Latham D. W., 2009 (in preparation)
- Hurley J.R., Pols O.R., Tout C.A., 2000 MNRAS, 315, 543
- Hurley J.R., Tout C.A., Pols O.R., 2002, MNRAS 329, 897
- Hurley J.R., Pols O.R., Aarseth S.J., Tout C.A., 2005, MNRAS, 363, 293
- Hut P., 1981, A & A, 99, 126
- Hut P., McMillan S., Goodman J., Mateo M., Phinney E. S., Pryor C., Richer H. B., Verbunt F., Weinberg M., 1992, PASP, 104, 981
- Kaluzny J., Mazur B., & Krzeminski W., 1993, MNRAS, 262, 49
- Kippenhahn R., Wiegert A., Hoffmeister R., 1967, in Alder B., Fernbach S., Rotenburg M., eds, Methods in Computational Physics, Vol. 7, Astrophysics. Academic Press, New York, p. 129
- Kroupa P., Tout C. A., Gilmore G., 1993, MNRAS, 262, 545 (KTG93)
- Levato H., 1974, A&A, 35, 259
- Marinović A.A., Glebbeek E., & Pols O.R., 2008, A&A, 480, 805
- Mathieu, R.D. 1983, PhD Thesis, California Univ., Berkeley
- Mathieu, R.D. 1985, IAUS, 113, 427, ed. J. Goodman, & P. Hut (Dordrecht: D Reidel Publishing)
- Mathieu R.D., & Latham D.W. 1986, AJ, 92, 1364
- Mathys G. 1987, A & AS, 71, 201
- McCrea, W.H., 1964, MNRAS, 128, 147

- Ostlie D.A., Carroll B.W. 2007, *An Introduction to Stellar Astrophysics*, 2nd ed., Addison Wesley
- Pols O. R., Marinus M., 1994, *A&A*, 288, 475
- Pols O.R., Schröder K.-P., Hurley J.R., Tout C.A., Eggleton P.P., 1998, *MNRAS*, 298, 525
- Portegies Zwart S. F., Verbunt F., 1996, *A&A*, 309, 179, (PZV)
- Sills A., Faber J. A., Lombardi J. C., Rasio F. A., Warren A. R., 2001, *ApJ*, 548, 323
- Spitzer, L. 1987, *Dynamical Evolution of Globular Clusters* (Princeton, NJ: Princeton Univ. Press)
- Stryker L.L., 1993, *PASP*, 105, 692
- Tout C. A., Aarseth S. J., Pols O. R., Eggleton P. P., 1997, *MNRAS*, 291, 732
- Wheeler J.C., 1979a, *ApJ*, 234, 569
- Whyte C. A., Eggleton P. P., 1985, *MNRAS*, 214, 357
- Xuefei C., Han Z., 2009, *MNRAS*,

